RSC Advances

PAPER

View Article Online
View Journal | View Issue

Cite this: *RSC Adv.*, 2015, **5**, 11397

Micellar solution with pH responsive viscoelasticity and colour switching property†

J. Linet Rose,[a] B. V. R. Tata,[b] Yeshayahu Talmon,[c] V. K. Aswal,[d] P. A. Hassan[e] and Lisa Sreejith*[a]

Received 10th November 2014
Accepted 5th January 2015

DOI: 10.1039/c4ra14195d

www.rsc.org/advances

Macroscopic properties of amphiphilic systems can be reversibly controlled by tailoring micellar morphology *via* appropriate choice of additive and external stimulus. In this work we report an aqueous micellar system showing pH responsive viscoelasticity and optical properties. pH sensitive behaviour of a phenolic acid, namely, *ortho*-coumaric acid (OCA) is effectively utilized to tune self-assembly in cetyltrimethylammonium bromide (CTAB) solution. Reversible switching between colourless, gel-like state and fluorescent green colour, liquid-like state can be attained by pH adjustment. pH dependent changes in bulk properties and the microstructures responsible for the behaviour were studied by means of rheology, UV-vis and fluorescence spectroscopic techniques, small angle neutron scattering (SANS) and cryogenic transmission electron microscopy (cryo-TEM). Rheological studies suggested transition between viscoelastic fluid and Newtonian liquid or *vice versa*, with specific changes in pH. Viscoelasticity of the system is attributed to the presence of entangled threadlike micelles. pH sensitive interactions between surfactant micelles and phenolic additive is regarded as the key factor regulating the morphological transitions and related flow behaviour in CTAB–OCA solution.

1. Introduction

The phenolic analogues of cinnamic acid are naturally occurring products distributed among a wide variety of plants. Relying on their ability to scavenge free radicals, development of anticancer drugs from phenolic acids is an active area of research.[1] Certain positional isomers of hydroxy cinnamic acid can act as strongly binding counter-ions which can dramatically modify the aggregation properties of surfactants in aqueous medium.[2] The unique properties of surfactant based micelles attract a great deal of interest due to their ease of preparation and reversible response to various external stimuli. There are ample works referring to the ability of strongly binding counter ions to modify effectively the viscoelastic properties of surfactant systems by aiding the elongation of micelles.[3–5] Threadlike ("wormlike") micelles are one of the most fascinating morphologies resulting from amphiphilic self-aggregation. Entanglement of long worms into a transient network can induce viscoelastic properties to the solution. The ability of entangled threadlike micelles (TLMs) to break and reform reversibly under shear enables their use in thickening and drag reducing applications.[6–8] Gel-like appearance with non-Newtonian flow behaviour makes wormlike micelles distinctive from their spherical analogues. Spherical micellar solution is characterized by water like fluidity and shear independent Newtonian viscosity.[9] Inter conversion between spherical and wormlike morphologies is generally accompanied with a dramatic shift in flow behaviour. The *ortho* isomer of hydroxy cinnamic acid (*ortho*-coumaric acid, OCA), when introduced to an aqueous micellar solution containing the cationic surfactant, cetyltrimethylammonium bromide (CTAB), showed the ability to increase the viscosity of the system significantly. Higher concentrations of the acid are capable of bringing viscoelasticity to the system. *Ortho*-coumaric acid, with an aromatic ring bearing two nearby polar substituents, can effectively bind to the palisade layer of surfactant micelles, thereby transforming the spherical micelle to threadlike geometry.

Recently there has been much interest in developing switchable TLMs for stimuli-responsive applications. External stimuli such as temperature, light, pH, redox coupling *etc.*, can reversibly control the flow properties by tailoring micellar morphology in solution.[10–15] Among those parameters, pH is of particular interest in industrial and pharmaceutical areas due to the ease of execution and quickness of reversibility. Most of the related reports involve the use of pH responsive polymeric hydrogels or synthetic amphiphiles bearing pH sensitive functional groups.[16,17] High cost, complexity of synthesis and low yield narrow down their

[a]*Department of Chemistry, NIT Calicut, Kerala, India. E-mail: lisa@nitc.ac.in; Fax: +91-495-22867280; Tel: +91-495-2286553*

[b]*Condensed Matter Physics Division, IGCAR, Kalpakkam, India*

[c]*Department of Chemical Engineering, Technion-Israel Institute of Technology, Haifa, 3200003, Israel*

[d]*Solid State Physics Division, BARC, Mumbai, India*

[e]*Chemistry Division, BARC, Mumbai, India*

† Electronic supplementary information (ESI) available. See DOI: 10.1039/c4ra14195d

practical applicability. pH-responsive wormlike micelles are nowadays getting accepted as simple and cost effective alternatives for strategies involving tedious synthetic procedures. Huang and co-workers have demonstrated the smart choice of different aromatic counter-ions for constructing switchable TLMs, active at different pH ranges.[18] This motivated us to inspect the possibility of developing the current system, comprising of CTAB and OCA as a pH tunable fluid. Interestingly, the system showed pH sensitive flow properties along with colour and fluorescence switching. The system can be switched between colourless, gel-like state and fluorescent green coloured, liquid-like state by pH adjustment.

In most of the pH switchable fluids fabricated through the incorporation of pH responsive additives to amphiphiles, the response is elicited in the form of perceptible changes in the flow behaviour. The use of phenolic additives to induce pH responsiveness to micellar fluid is not much discussed in the literature. In strongly alkaline medium, phenolic compounds tend to exist as phenoxide ion which alters the extent of aqueous solubilisation and mode of interaction with surfactant micelles.[19] In addition, phenoxide ions induce colour and fluorescence properties to the system which can be modulated *via* pH. Since phenoxide formation is a strong function of pH, the mode of surfactant–additive interaction and optical properties of the solution can be controlled through pH adjustments. Thus, phenolic compounds are attractive additives to surfactant solutions to design smart fluids showing duel response to pH changes. In the present study *ortho*-coumaric acid is specifically selected because of its structural similarity to strongly binding counter ions. No complex synthesis is required to incorporate pH sensitive moiety to the surfactant micelles. pH triggered changes in viscoelasticity and optical properties were investigated by means of rheology, UV-vis and fluorescence spectroscopic techniques. Self-assembled structures, responsible for the changes in flow properties were identified using small angle neutron scattering (SANS) and cryogenic transmission electron microscopy (cryo-TEM).

2. Experimental section

2.1 Materials

Cetyltrimethylammonium bromide (CTAB) and *ortho*-coumaric acid (OCA) were purchased from BDH England (99% assay) and Alfa Aesar England (99.5% assay) respectively. All the chemicals were used as received. Samples were prepared in deionized Milli-Q water and kept in a water bath at 45 °C with stirring for about one hour for homogeneity. The resulting samples were stored at room temperature for at least one day before running experiments. pH of the solution was adjusted by adding micro volumes of aqueous solutions of NaOH or HCl (Nice Chemicals, India) and measured using Systronics digital pH meter-335 (±0.01). Scheme 1 shows the chemical structures of CTAB and OCA.

2.2 Rheological measurements

Rheological measurements were performed on an MCR-301 rheometer (Anton Paar, Germany) with a parallel plate (50 mm diameter) or double gap cylindrical measuring system. Sample

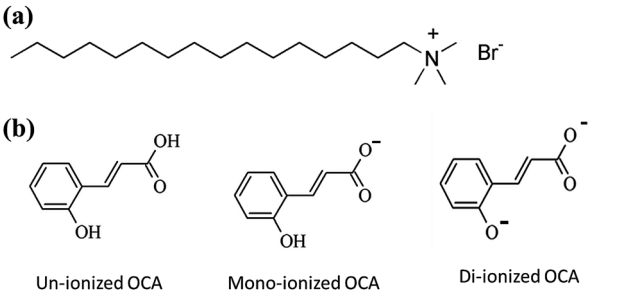

Scheme 1 Chemical structures of (a) cetyltrimethylammonium bromide and (b) *ortho*-coumaric acid.

temperature was maintained to the accuracy of ±0.01 °C. The viscosities of samples were obtained from steady shear measurements with shear rate ranging from 0.001–100 s^{-1}. Dynamic frequency spectra were obtained in the linear viscoelastic regime of each sample as determined by strain sweep measurements. Frequency sweep measurements were performed in the angular frequency range of 0.05–100 rad s^{-1}. All the measurements reported here were carried out at 30 °C.

2.3 UV-vis spectroscopy

UV-visible spectra were recorded on a double beam spectrophotometer (Systronics, 2202) at room temperature, using quartz cuvette.

2.4 Fluorescence spectroscopy

Fluorescence spectra of surfactant solutions at different pH values were obtained with LS 45 fluorescence spectrometer (PerkinElmer) at room temperature. The excitation wavelength used was 385 nm.

2.5 SANS

SANS experiments were carried out using SANS diffractometer at Dhruva Reactor, Bhabha Atomic Research Centre, Trombay. The mean wavelength of the incident neutrons is 5.2 Å and the angular distribution of the scattered neutrons were recorded using a one dimensional position sensitive detector. The diffractometer covers the scattering wave vector, q range of 0.017–0.032 $Å^{-1}$. The sample was loaded in a quartz cell of 0.5 cm path length and in all the measurements the temperature was kept fixed at 30 °C. The differential scattering cross section per unit volume, $I(q)$ of the sample was determined from the measured scattered neutron intensity as per the standard procedure.[20]

2.6 Cryo-TEM

Vitrified cryo-TEM specimens were prepared in a controlled environment vitrification system (CEVS), at a controlled temperature and fixed relative humidity (100%). It is followed by quenching into liquid ethane at its freezing point. The specimens, kept below −178 °C, were examined by an FEI T12 G2 transmission electron microscope, operated at 120 kV, using a Gatan 626 cryo-holder system. Images were recorded digitally

in the minimal electron dose mode by a Gatan US1000 high resolution cooled CCD camera with the digital micrograph software package.

3. Results and discussion

3.1 Rheological studies

Flow properties of surfactant solution depend strongly on the morphology of aggregates present in the system. It is well known that the cationic surfactant CTAB forms spherical micelles in aqueous medium and shows water-like viscosity, at relatively low surfactant concentration.[21] Strongly binding additives can viscosify CTAB solution by bringing the elongation of micelles. OCA is an aromatic additive with sparing solubility in water.[22] But aqueous solubility of OCA was enhanced considerably in presence of CTAB micelles. In addition, the viscosity of CTAB solution was found to increase with successive increase in the concentration of OCA. The effect of OCA concentration on the steady shear rheology of a fixed concentration of CTAB solution (100 mM) is presented in Fig. 1. Samples with low OCA concentration showed shear independent Newtonian flow behaviour and viscosity comparable with that of water. On increasing the additive concentration, the zero shear viscosity was found to increase and samples with relatively high OCA concentration exhibited shear thinning behaviour at high shear rates. Shear thinning behaviour is an indication of the existence of transiently networked structures in the system which can undergo reversible disruption under shear.[23] The transient mesh resulting from the entanglement of long micelles (TLMs) can bring viscoelastic properties to the system.

Viscoelastic nature of micelle solution can be better inferred from the dynamic rheological measurements. TLMs are typical examples for Maxwell fluids with single relaxation time. The variation of elastic modulus (G') and viscous modulus (G'') with oscillatory shear frequency (ω) for Maxwellian fluids is given as

$$G' = \frac{\omega^2 {\tau_R}^2}{1+\omega^2 {\tau_R}^2} G_0 \quad G'' = \frac{\omega \tau_R}{1+\omega^2 {\tau_R}^2} G_0 \qquad (1)$$

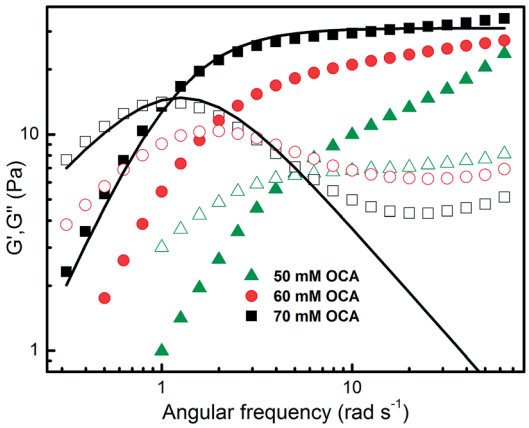

Fig. 2 Oscillatory shear rheology of 100 mM CTAB/x mM OCA samples with relatively high OCA concentration. Filled symbols represent G' and open symbols represent G''. Solid line is a fit to Maxwell model.

where G_0 is the plateau modulus (steady value of G' at high frequency) and τ_R is the relaxation time.[24] Oscillatory shear rheology at three different additive concentrations is shown in Fig. 2. A remarkable shift in the cross over frequency (ω_c, frequency at which G' and G'' cross) towards low frequency region can be seen with increase in additive concentration. This signifies an increase in relaxation time ($\tau_R = 1/\omega_c$), which in turn, hints the elongation of micelles. Data obtained for 100 mM CTAB/70 mM OCA was fitted to Maxwell equations. Though the fit is not excellent, typical pattern, exhibiting a viscous nature at low ω and an elastic nature at high ω with a plateau for G' and minimum for G'', is closely followed by sample. Such behaviour was not strictly followed by samples with lower OCA concentration. Shear thinning behaviour observed in the steady shear rheology along with the Maxwell type pattern obtained in the oscillatory shear measurement suggest that high concentration of OCA is capable of inducing viscoelasticity to 100 mM CTAB solution by aiding the elongation of micelles. Adjacent

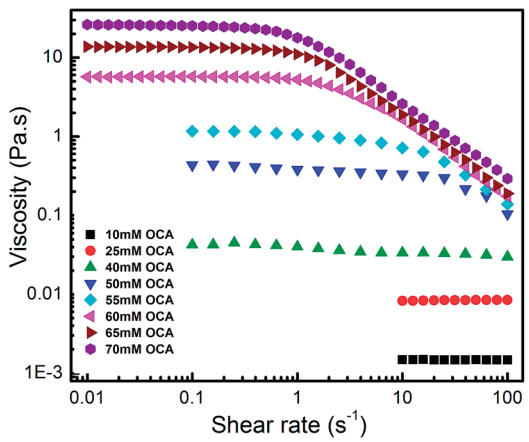

Fig. 1 The steady shear rheological response of 100 mM CTAB/x mM OCA system at varying concentrations of OCA.

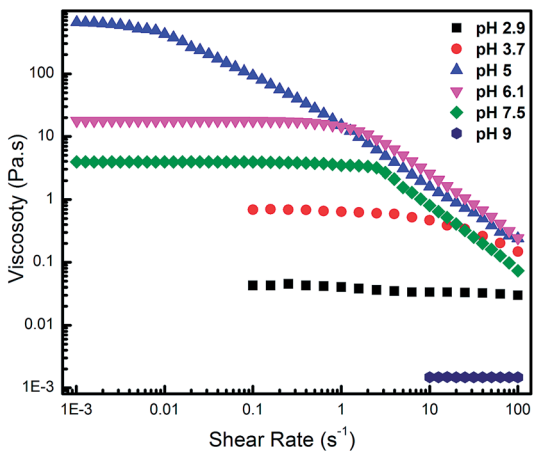

Fig. 3 The steady shear rheological response of 100 mM CTAB/40 mM OCA sample at different pH values.

positioning of two polar functional groups (carboxyl and hydroxyl groups) on the aromatic ring enables the strong binding of OCA molecules to CTAB micelles.[25] Binding of sufficient number of additive molecules offers effective charge screening to cationic micelles and bring micellar elongation.

100 mM CTAB/40 mM OCA sample, with relatively low viscosity but sufficient additive concentration to show pronounced response to pH, was chosen in order to investigate the effect of pH on CTAB–OCA micellar system. The steady shear rheology of the sample at different pH values is presented in Fig. 3. At pH 2.9, the sample showed relatively low viscosity ($\approx$0.04 Pa s). On increasing the solution pH to 5, huge increase in viscosity ($\approx$600 Pa s) and an explicit shear thinning non-Newtonian flow pattern were observed. However on further increase in pH to 9, a significant drop in viscosity ($\approx$0.001 Pa s) occurred, and the sample followed shear-independent Newtonian flow pattern.

When 100 mM CTAB/40 mM OCA sample is at and around its native pH ($\approx$2.9), OCA molecules are only weakly ionised and poor electrostatic interaction with CTAB micelles is expected. In addition, the selected concentration of OCA is not sufficient to bring strong viscoelasticity to the system *via* hydrophobic interaction. So the morphology at this pH is limited to ellipsoidal/short cylindrical micelles, which is manifested as the low viscosity and nearly Newtonian flow behaviour of the system at low pH values. The carboxylic acid group of OCA can be ionised depending on the solution pH. Progressive deprotonating of OCA molecules take place on increasing the pH by adding NaOH.[26] More ionised molecules can offer better charge screening to cationic surfactant heads. With the aromatic ring and ionised carboxylic acid group, OCA can bind more effectively to CTAB micelles through both hydrophobic effect and electrostatic attraction which leads to micellar elongation and eventually brings viscoelasticity to the system. This is evident from the increase in viscosity of 100 mM CTAB/40 mM OCA sample with increase in pH.

Very high viscosity and viscoelasticity observed for the sample around pH 5 can be explained in terms of the pK_a value of OCA (=4.61).[27] Above pK_a, major fraction of OCA molecules exists as carboxylate anions. Hence maximum CTAB–OCA interaction occurs around pH 5. Shear thinning behaviour observed for 100 mM CTAB/40 mM OCA sample at pH 5 suggest the presence TLMs in the system. The dynamic rheology of the sample at this pH (Fig. 4) satisfactorily fits with Maxwell behaviour which confirms the presence of TLMs.

Some fascinating changes were observed on increasing the pH further to alkaline range. Colourless sample turned green and viscosity started decreasing with successive increase in pH beyond 5. Shear thinning behaviour disappeared around pH 9 and the sample exhibited Newtonian flow pattern (Fig. 3) with viscosity close to that of water ($\approx$0.001 Pa s). Maxwell behaviour was poorly followed by the sample at alkaline pH. A shift in the cross over frequency towards high frequency region was observed in the dynamic rheology of 100 mM CTAB/40 mM OCA sample on increasing the pH beyond 5 (Fig. 4). This signifies an increase in fluidity and hence the reduction in micellar length. Thus, the sample is switched from a viscoelastic fluid to watery liquid on increasing the pH from 5 to 9. This switching can be reversibly controlled by modulating the pH between 5 and 9 by the addition of minute volumes of aqueous NaOH or HCl.

Different mechanisms such as second dissociation of dibasic additive,[18] quarternization of tertiary amine group attached to the surfactant,[28] variations in the net charge of amino acid type additives[29] *etc.*, were proposed to explain the pH-switchable flow properties in aqueous micellar solution. In most of such reported systems the authors suggested pH sensitive threadlike to spheroidal/short cylindrical micellar transition as the physical reason behind the drastic viscosity drop. The additive used in the present system is a phenolic acid bearing both –COOH and –OH functional groups. In alkaline solution, phenolic compounds tend to exist in the phenoxide form due to the possibility of resonance stabilization. Hence the reversible formation of phenoxide ions in basic medium could be the plausible chemistry behind the observed viscosity-drop in CTAB–OCA system at elevated pH values. The better aqueous solubility of phenoxide ions lead to progressive leaching out of additive molecules from the micellar surface to the surrounding medium upon increasing the pH. This will either result in shortening of micellar length, or makes the system more flexible by catalysing entanglement scission.[30]

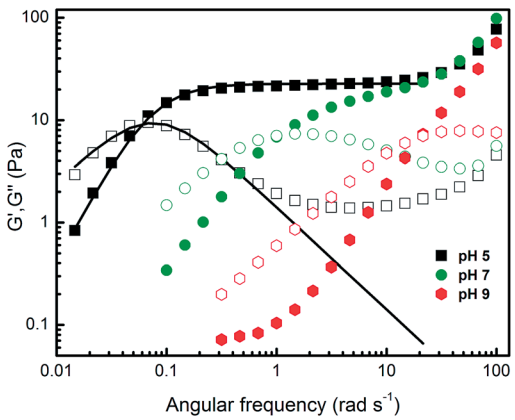

Fig. 4 Dynamic rheology of 100 mM CTAB/40 mM OCA sample at three different pH values. Filled symbols represent G' and open symbols represent G''. Solid line is a fit to Maxwell model.

3.2 Spectroscopic studies

The macroscopic appearance of the sample at different pH values is shown in Scheme 2. In acidic pH range, sample appeared colourless. On increasing the pH to the alkaline range, sample changed to a fluorescent green coloured liquid. UV-visible spectrum of the sample at different pH values is presented in Fig. 5. Two absorption peaks were observe in the acidic pH, one at 271 nm and the other at 317 nm. No characteristic absorption was observed in the visible region. Both n $\rightarrow$ π^* and $\pi \rightarrow \pi^*$ transitions are expected in phenolic acids.[31] The absorption peak at 317 nm could be due to the presence of unsaturated carboxylic acid group on the benzene ring in OCA. On increasing the pH to the alkaline range, the absorption peak at 317 nm exhibited a red shift towards the visible region, and

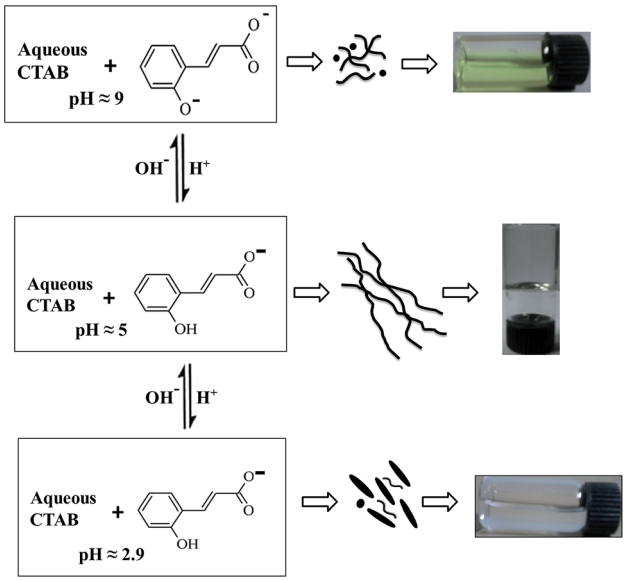

Scheme 2 Changes in additive structure, micellar morphology and macroscopic appearance of the sample with pH variation.

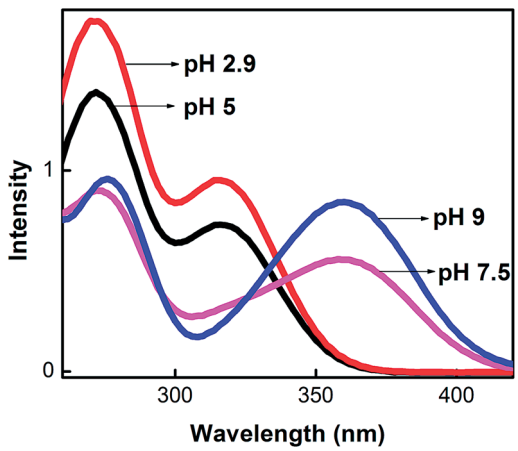

Fig. 5 UV-vis spectra of diluted solutions of 100 mM CTAB/40 mM OCA at different pH values.

the sample changed to a water-like liquid with fluorescent green colour.

The variation in fluorescence emission of the sample at different pH values are plotted in Fig. 6. At pH 2.9, a weak fluorescence emission was observed at 437 nm (when excited at 385 nm). A red shift in fluorescence emission was noticed on increasing the pH by adding minute volumes of NaOH. Beyond pH 5, an additional fluorescence emission peak was observed at 490 nm. On further increase in pH, the emission intensity of peak at 490 nm increased, whereas the peak at 437 nm diminished. Above pH 7, only the peak at 490 nm persisted, and showed continuous increase in intensity with pH. In short, the sample progressed from nearly colourless, viscoelastic fluid to deep fluorescent green coloured, viscous liquid upon increasing the pH from 5 to 9. Both the red shift in absorption and the

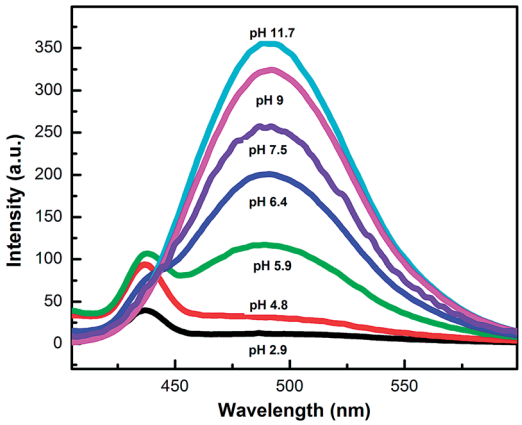

Fig. 6 Fluorescence emission spectra of diluted solutions of 100 mM CTAB/40 mM OCA at different pH values.

successive increase in intensity observed in the fluoresce emission of CTAB–OCA samples upon increasing the pH suggest phenoxide formation and resonance stabilization. Phenoxide ions formed in alkaline solution, together with the unsaturated carboxylate group, extend the conjugation on OCA considerably, and shift the absorption towards the visible region. This contributes towards the coloured appearance and enhanced fluorescence at high pH.

Both the rheological properties and fluorescence of the system can be reversibly controlled by the addition of minute volumes of NaOH or HCl. Fig. 7 shows the variation of zero shear viscosity and fluorescence emission intensity by reversible control of pH between 5 and 9. The system retains its viscosity and fluorescence without much deviation even after being switched three times.

3.3 SANS studies

pH dependent changes in the flow behaviour of CTAB–OCA micellar solution, as inferred from rheological studies, strongly

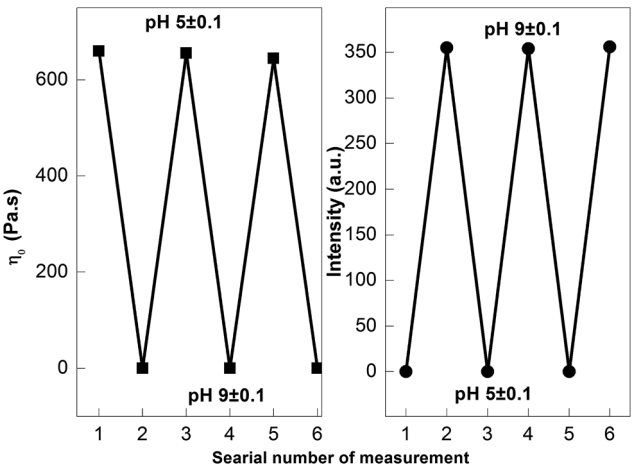

Fig. 7 Change in zero shear viscosity (measured at 30 °C) and fluorescence emission intensity (at 490 nm) of sample during repeated cycles of pH variation.

suggest morphological transitions in the microscopic level. In order to investigate the structural features, SANS measurements were performed at selected pH values. Fig. 8 shows the SANS spectra obtained for 100 mM CTAB/40 mM OCA sample at different pH values. The spectra at pH 2.9 shows a correlation peak in the low q region (at $q \sim 0.032$ Å^{-1}) which is an indication of repulsive interaction between charged micellar heads.[32] An increase in the scattering intensity and disappearance of correlation peak were seen at pH 5, which strongly suggest scattering from well screened and elongated micelles. Re-appearance of a broad peak, indicating some modifications in the micellar interaction, was observed at pH 9. Prolate ellipsoidal model was used for the analysis of SANS data. For mono disperse micelles, the coherent differential scattering cross section $d\Sigma/d\Omega$ is given by the equation[33,34]

$$d\Sigma/d\Omega = n(\rho_m - \rho_s)^2 V^2[\langle F(q)^2\rangle + \langle F(q)\rangle^2(S(q) - 1)] + B \quad (2)$$

where n is the number density of micelles, ρ_m and ρ_s are scattering length densities of micelle and solvent respectively and V is the volume of the micelle. $F(q)$ is the single particle form factor and $S(q)$ is the inter-particle structure factor. B is a constant that represents the incoherent scattering background. For ellipsoidal micelles, the single particle form factor can be obtained from[35,36]

$$\left\langle F(q)^2\right\rangle = \int_0^1 \left[F(q,\ \mu)^2 d\mu\right] \quad (3)$$

$$\langle F(q)\rangle^2 = \left[\int_0^1 F(q,\mu)d\mu\right]^2 \quad (4)$$

$$F(q,\mu) = \frac{3(\sin x - x\ \cos x)}{x^3} \quad (5)$$

$$x = q[a^2\mu^2 + b^2(1 - \mu^2)]^{1/2} \quad (6)$$

where a and b are the semi-major and semi-minor axis of the ellipsoidal micelle respectively and m is the cosine of the angle between the directions of a and the wave vector transfer q. The inter-particle structure factor $S(q)$ specifies the correlation between the centres of different micelles and is the Fourier transform of the radial distribution function $g(r)$ for the mass centre of the micelle. The calculation of $S(q)$ for any shapes other than spheres is complicated. Hence, for $S(q)$ calculations, prolate ellipsoidal micelles are assumed to be a rigid equivalent spheres of diameter $\sigma = 2(ab^2)^{1/3}$ interacting through a screened Coulomb potential. The dimensions of micelle were determined from the model fitting of SANS data. The values of semi minor axis ($b = 20$ Å) and semi major axis ($a = 45$ Å) obtained from large q data analysis of the SANS spectrum of 100 mM CTAB/40 mM OCA sample at pH 2.9 suggest the presence of ellipsoidal micelles in the system. A considerably high value of semi major axis ($a \approx 164$ Å) was obtained for the sample at pH 5. But the semi minor axis ($b = 20$ Å) remained unaltered, which supports the uniaxial elongation of micelles. On increasing the pH further to 9, a decrease in the semi major axis to 65 Å, hinting a reduction in micellar length, was observed. When TLMs with length longer than a few tens of nanometers are formed by one-dimensional elongation, the main feature of SANS spectra is limited to the cross-sectional radius of the micelle.[27] So the values obtained for semi-major axis may not match with the exact length of the TLM. However, the observed spectral features and trend of calculated micellar dimensions, strongly support the notion of pH induced structural transitions in the system.

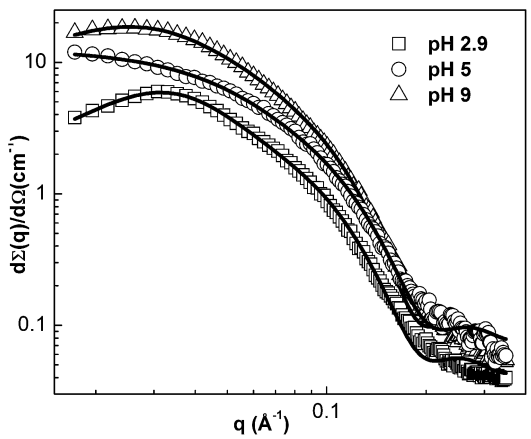

Fig. 8 SANS profiles of 100 mM CTAB/40 mM OCA sample at different pH values (measured at 30 °C). Solid line represents fit to the model used for data analysis.

3.4 Cryo-TEM observation

Transmission electron microscopy under cryogenic conditions is the most desirable technique for the direct visualisation of micellar morphology.[37] From the results of rheological investigation it is clear that mode of CTAB–OCA interaction and subsequent micellar elongation depend on the extent of aqueous ionisation of OCA molecules. Aqueous ionisation in turn, is a strong function of pH of the medium. The progressive increase in the zero shear viscosity of the system up to around first pK_a of OCA strongly supports this notion and suggests structural progression from ellipsoidal/short cylindrical micelles to long TLMs on increasing the pH till pK_a. The smart feature of the system *i.e.*, reversible switching between colourless, viscoelastic fluid and fluorescent water like liquid, occurs beyond first pK_a. SANS results indicate that aggregates at pH 9 are shorter than those at pH 5. According to the literature viscosity reduction beyond peak viscosity can be due to various reasons such as micellar shortening/disintegration,[38] branching of TLMs,[39] increased concentration of free counter ions in the bulk phase making the TLMs more flexible[30] *etc.* So in order to confirm unambiguously the structural transition responsible for the switching between gel-like and water-like state with in the pH range 5–9, we carried out the cryo-TEM imaging at pH 5 and pH 9. The images are presented in Fig. 9. Very long micelles responsible for the high viscosity and viscoelasticity of sample can be clearly seen at pH 5 (Fig. 9a). TLMs are aligned along the shear flow due to sample preparation procedure. Spheroidal micelles or micellar end caps are rarely observed in the imaged area. At pH 9, network of highly flexible and overlapped micelles

are present in the sample. Several dark spots are also visible which could be either spherical micelles or TLM end caps. This suggests that micelle length has reduced on increasing the pH to 9. These observations are in qualitative agreement with the SANS results. Considerably high value of semi-major axis and absence of correlation peak in the SANS spectrum obtained for the sample at pH 5 suggest scattering form long micelles. Reduction in semi-major axis and appearance of a broad peak in the SANS spectrum on increasing the pH to 9 are consistent with the presence of shortened micelles.

Cryo-TEM image confirms that the shear thinning flow behaviour and Maxwell-like rheology observed for the sample at pH 5 are due to the presence of very long TLMs which can align under shear.

The zero shear viscosity of the sample at pH 9 ($\approx$0.001 Pa s) is similar to that of purely spherical micellar solution. But the cryo-TEM image of the sample revels that the system is not fully devoid of TLMs. Spherical aggregates are coexisting with flexible TLMs. So in addition to shortening of micelles, the increased flexibility of TLMs could also contribute towards the reduction in viscosity. One mechanism that has been proposed to explain the drop in viscoelastic properties of TLMs is the 'ghost-like crossing' through entanglement point.[40–42] According to this model, TLMs can pass one another *via* fusion at the entanglement positions. This process is catalysed by the collision of free counter ions in the bulk phase with TLMs. Thus increased concentration of counter ion in the bulk phase quickens the relaxation process (reduces τ_R) leading to a drop in viscoelasticity. As discussed earlier, phenoxide ions formed in the alkaline solution tend to desorb from micelle surface into surrounding water medium there by increasing the counter ion concentration in the bulk than on micellar surface. This, in addition to cause shortening of micelles, promotes the ghost-like crossing mechanism. Water-like viscosity and Newtonian flow pattern exhibited by the 100 mM CTAB/40 mM OCA sample at pH 9, in spite of the presence of a significant proportion of TLMs as observable in the cryo-TEM image, support this opinion.

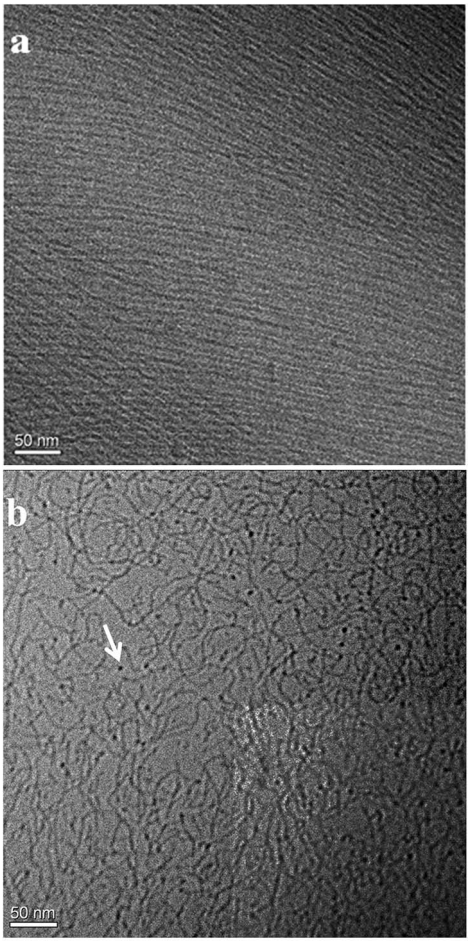

Fig. 9 Cryo-TEM images of 100 mM CTAB/40 mM OCA sample at (a) pH 5 and (b) pH 9 (scale bar: 50 nm, spherical micelle is indicated using arrow in b).

Changes in additive structure and micellar morphology responsible for the pH tunable behaviour of 100 mM CTAB/40 mM OCA sample is summarised in Scheme 2. Relatively low viscosity, nearly shear independent flow behaviour and the SANS profile of the sample indicate the presence of ellipsoidal micelles as the predominant morphology at and around pH 2.9. Rheological results and cryo-TEM observation strongly suggest the existence of long TLMs, inducing high viscosity and viscoelasticity to the sample, at pH 5. As the pH is around the pK_a of OCA, maximum ionisation and micellar binding is expected. Non-readily flowing nature of the sample at pH 5, in an inverted vial, can be seen from the photograph. Colour and fluorescence property exhibited by the sample in alkaline medium suggest the existence of OCA in the phenoxide form. Cryo-TEM image revealed the coexistence of spherical micelles and TLMs in the sample at pH 9. Better aqueous solubility of phenoxide ions contributes towards reduction in micellar length and increased flexibility of TLMs. Since the extent of ionisation and micellar binding of OCA depend on solution pH, aggregate morphology and bulk properties of CTAB–OCA micellar solution can be tuned by pH adjustments.

4. Conclusions

Manipulation of micellar morphology and properties like rheology, fluorescence *etc.*, by simple tuning of pH, reported in this work, is facile and cost effective. Both the surfactant and additive used are easily available, and the production of switchable micelles in the system needs no complicated synthetic procedure. In addition, the counter-ion used in the system possesses native fluorescence and interesting pharmacological activities. The novelty of the system lies in the colour and fluorescence switching observed along with the viscosity changes. The sample changes from colourless viscoelastic fluid to strongly fluorescent liquid on increasing the pH from 5 to 9. Using rheology, UV-vis spectroscopy, fluorescence spectroscopy, cryo-TEM and SANS, it was hypothesised that the pH responsiveness originates from phenoxide formation and subsequent leaching out of counter ions from micellar interface favouring the formation of highly flexible micelles. pH switchable TLMs are widely used for industrial formulations, such as drag

reducing agents, thickeners *etc.* TLMs with native fluorescence switching properties are rarely reported in the literature. Since the additive used is anti-oxidative, proper replacement of the current surfactant with non-cytotoxic analogues will make the system biocompatible, and will enable different kinds of biomedical applications.[43,44]

Acknowledgements

This work was performed under the collaborative research scheme (CRS-K-0/5/20) of the UGC-DAE Consortium for Scientific Research, Kalpakkam node, India. The support and encouragement of Dr G. Amarendra (scientist-in-charge, Kalpakkam node) is gratefully acknowledged. The cryo-TEM work was performed at the Laboratory for cryo-EM of Soft Matter, supported by the Technion Russell Berrie Nanotechnology Institute (RBNI). Authors are thankful to Dr Ellina Kesselman and Dr Judith Schmidt (Technion-Israel Institute of Technology) for their immense help in the cryo-TEM analysis and Dr Lakshmi C (Bio-organic lab., Dept. of Chemistry, NIT Calicut) for providing the fluorescence spectroscopy facility. Thanks are due to Dr K. Saravanakumar (IGCAR, Kalpakkam), for his help in carrying out the rheological experiments, Mr Abhineesh Babu and Mr. Shyvindraj. U.P (Dept. of Chemistry, NIT Calicut), for carrying out the fluorescence measurements.

Notes and references

1 P. De, M. Baltas and F. Bedos-Belval, *Curr. Med. Chem.*, 2011, **18**, 1672.
2 A. Heins, V. Garamus, B. Steffen, H. Stöckmann and K. Schwarz, *Food Biophys.*, 2006, **1**, 189.
3 H. Rehage and H. Hoffmann, *J. Phys. Chem.*, 1988, **92**, 4712.
4 B. K. Roy and S. P. Moulik, *Curr. Sci.*, 2003, **85**, 1148.
5 C. Oelschlaeger, M. Schopferer, F. Scheffold and N. Willenbacher, *Langmuir*, 2009, **25**, 716.
6 J. F. Berret, *Molecular Gels*, Springer, Netherlands, 2006, p. 667.
7 J. Yang, *Curr. Opin. Colloid Interface Sci.*, 2002, **7**, 276.
8 H. Shi, Y. Wang, B. Fang, Y. Talmon, W. Ge, S. R. Raghavan and J. L. Zakin, *Langmuir*, 2011, **27**, 5806.
9 S. A. Kumar, Z. Naqvi and Kabir-ud-Din, *Langmuir*, 2000, **16**, 5252.
10 T. S. Davies, A. M. Ketner and S. R. Raghavan, *J. Am. Chem. Soc.*, 2006, **128**, 6669.
11 H. Sakai, Y. Orihara, H. Kodashima, A. Matsumura, T. Ohkubo, K. Tsuchiya and M. Abe, *J. Am. Chem. Soc.*, 2005, **127**, 1345.
12 A. M. Ketner, R. Kumar, T. S. Davies, P. W. Elder and S. R. Raghavan, *J. Am. Chem. Soc.*, 2007, **129**, 1553.
13 H. Maeda, A. Yamamoto, M. Souda, H. Kawasaki, K. S. Hossain, N. Nemoto and M. Almgren, *J. Phys. Chem. B*, 2001, **105**, 5411.
14 H. Kawasaki, M. Souda, S. Tanaka, N. Nemoto, G. Karlsson, M. Almgren and H. Maeda, *J. Phys. Chem. B*, 2002, **106**, 1524.
15 K. Tsuchiya, Y. Orihara, Y. Kondo, N. Yoshino, T. Ohkubo, H. Sakai and M. Abe, *J. Am. Chem. Soc.*, 2004, **126**, 12282.
16 K. J. C. van Bommel, C. van der Pol, I. Muizebelt, A. Friggeri, A. Heeres, A. Meetsma, B. L. Feringa and J. van Esch, *Angew. Chem., Int. Ed.*, 2004, **43**, 1663.
17 S. L. Zhou, S. Matsumoto, H.-D. Tian, H. Yamane, A. Ojida, S. Kiyonaka and I. Hamachi, *Chem.–Eur. J.*, 2005, **11**, 1130.
18 Y. Lin, X. Han, J. Huang, H. Fu and C. Yu, *J. Colloid Interface Sci.*, 2009, **330**, 449.
19 M. B. Smith and J. March, *Advanced Organic Chemistry: Reactions, Mechanisms, and Structure*, Wiley-Interscience, New York, 6th edn, 2007, ISBN: 0-471-7209.
20 V. K. Aswal and P. S. Goyal, *Curr. Sci.*, 2000, **79**, 947.
21 Z. Lin, J. J. Cai, L. E. Scriven and H. T. Davis, *J. Phys. Chem.*, 1994, **98**, 5984.
22 2-Hydroxycinnamic acid; MSDS no. SC-238081 [online], Santa Cruz Biotechnology, Inc., Texas, USA, April 3, 2009, http://datasheets.scbt.com/sc-238081.pdf.
23 D. P. Acharya, D. Varade and K. Aramaki, *J. Colloid Interface Sci.*, 2007, **315**, 330.
24 P. A. Hassan, J. Narayanan and C. Manohar, *Curr. Sci.*, 2001, **80**, 980.
25 K. Bijma, E. Rank and J. B. F. N. Engberts, *J. Colloid Interface Sci.*, 1998, **205**, 245.
26 V. Patel, N. Dharaiya, D. Ray, V. K. Aswal and P. Bahadur, *J. Colloid Interface Sci.*, 2014, **455**, 67.
27 P. Yadav, H. Mohan, B. S. M. Rao and J. P. Mittal, *J. Chem. Sci.*, 2002, **114**, 721.
28 Z. Chu and Y. Feng, *Chem. Commun.*, 2010, **46**, 9028.
29 G. Verma, V. K. Aswal and P. Hassan, *Soft Matter*, 2009, **5**, 2919.
30 K. R. Francisco, M. A. da Silva, E. Sabadini, G. Karlsson and C. A. Dreiss, *J. Colloid Interface Sci.*, 2010, **345**, 351.
31 M. Butnariu, *Ann. Agric. Environ. Med.*, 2014, **21**(1), 11.
32 D. Varade, T. Joshi, V. K. Aswal, P. S. Goyal, P. A. Hassan and P. Bahadur, *Colloids Surf., A*, 2005, **259**, 95.
33 J. B. Hayter and P. Penfold, *Colloid Polym. Sci.*, 1983, **261**, 1022.
34 E. Y. Sheu, C. F. Wu and S. H. Chen, *J. Phys. Chem.*, 1986, **90**, 4179.
35 J. B. Hayter and P. Penfold, *Mol. Phys.*, 1981, **42**, 109.
36 J. P. Hansen and J. B. Hayter, *Mol. Phys.*, 1982, **46**, 651.
37 Y. Talmon, *Giant micelles – Properties and applications*, CRC press, 2007, p. 163.
38 S. R. Raghavan, H. Edlund and E. W. Kaler, *Langmuir*, 2002, **18**, 1056.
39 C. Oelschlaeger, M. Schopferer, F. Scheffold and N. Willenbacher, *Langmuir*, 2008, **25**, 716.
40 T. Shikata, H. Hirata and T. Kotaka, *Langmuir*, 1988, **4**, 354.
41 T. Shikata, M. Shiokawa and S. Imai, *J. Colloid Interface Sci.*, 2003, **259**, 367.
42 N. K. Pokhriyal, J. V. Joshi and P. S. Goyal, *Colloids Surf., A*, 2003, **218**, 201.
43 K. Rajagopal, D. A. Christian, T. Harada, A. Tian and D. E. Discher, *Int. J. Polym. Sci.*, 2010, **2010**, 379286, DOI: 10.1155/2010/379286.
44 G. H. Gao, Y. Li and D. S. Lee, *J. Controlled Release*, 2013, **169**, 180.

